DOI: 10.1002/chem.201103421

From Low to Very High Birefringence in Bis(2-pyridylimino)isoindolines: Synthesis and Structure–Property Analysis

Edwin W. Y. Wong, Jeffrey S. Ovens, and Daniel B. Leznoff*[a]

Abstract: A series of new substituted 1,3-bis(2-pyridylimino)isoindolines—1,3-bis(2-pyridylimino)-5,6-bis(2,6-diisopropylphenoxy)isoindoline (**2b**), 1,3-bis(2-pyridylimino)-5,6-bis(4-*tert*-butylphenyl)isoindoline (**2c**), and 1,3-bis(2-pyridylimino)-5-*tert*-butylisoindoline (**2d**)—were synthesized and structurally characterized by single-crystal X-ray diffraction. The birefringence (Δn) of the crystals of unsubstituted 1,3-bis(2-pyridylimino)isoindoline (**2a**), **2b**, **2c**, and **2d** were measured and found to vary greatly, with Δn values of 0.0654(3), 0.0629(17), 0.588(10), 0.701(12), respectively. A structure–property relationship for the birefringence values of **2a**–**2d** was outlined and indicated that the anisotropy of the polarizability of the molecules plays a crucial role in the birefringence of the crystals. The greatest birefringence values are achieved when the molecules are oriented in a face-to-face configuration intermolecularly, and along the crystallographic face being measured.

Keywords: birefringence · crystal engineering · optical properties · structure–property relationships · supramolecular chemistry

Introduction

Birefringent materials (the refractive index of which depends on crystallographic direction) have a wide range of applications such as optical filters,[1,2] waveplates,[3] and liquid-crystal displays.[4–6] Inorganic minerals, such as calcite and quartz, have been particularly widely employed for these purposes due to a high birefringence value in the case of calcite ($\Delta n = 0.172$), and the ability to cut large crystals of these materials for applications.[7–10]

Organic crystalline solids are also known to be birefringent. For instance, crystals of urea have a substantial value of $\Delta n = 0.118$.[11,12] For many organic crystals, the face-dependent refractive indices (and therefore the birefringence) were measured in the early-to-mid 1900s by using refractive-index-matching oils and/or prism coupling methodologies,[13] and over 2000 measurements have been tabulated and compiled.[11] The values are generally below $\Delta n = 0.2$; a very small number are greater than 0.5.[14,15] However, despite this plethora of measurement data and a good understanding of molecular polarizabilities, a chemical and crystallographic perspective regarding the 3D structural features that influence the birefringence properties has received very little attention.[16,17]

At the interface of the inorganic salts and organic compounds lies the realm of coordination polymers, which provide a Lego® building-block approach to designing new materials.[18–20] Recently, we have described how to rationally design coordination polymers with very high birefringence values.[21–24] These high values arise from a polymer framework that supports a set of anisotropic, highly polarizable ligands, such that their individual polarizability anisotropies build upon one another. Using the highly anisotropic 2,2′:6′,2″-terpyridine (terpy) ligand on a Pb/$[Au(CN)_2]^-$ framework, we were able to achieve values approaching $\Delta n = 0.5$.[22,23] Such a high value arises from the face-to-face arrangement of the terpy ligands, organized in this fashion by the coordination polymer framework. Terpy itself does not form good quality crystals for either of its two polymorphs, and neither polymorph shows the alignment required for a high birefringence value.[25,26]

In order to expand on this methodology, we began to explore bis(2-pyridylimino)isoindoline, or "lobsterate" (Lb)-based ligands (so named by us because of their resemblance to a lobster). Much like terpy, these are flat ligands built up of aromatic substituents, and would be expected to have a very high anisotropic polarizability as well. Furthermore, their transparency above 450 nm facilitates optical applications.

However, these isoindoline molecules, unlike terpy, do form good quality crystals. Depending on the R-group substituent, the majority have their molecules aligned face-to-face in their crystal structure, thus fulfilling one condition needed for high birefringence. Thus, the synthesis, structures, and birefringence measurements on a series of lobsterate molecules is outlined below and the birefringence correlated to the 3D packing array of the materials.

[a] E. W. Y. Wong, J. S. Ovens, D. B. Leznoff
Department of Chemistry, Simon Fraser University
8888 University Drive, Burnaby, BC, V5A 1S6 (Canada)
Fax: (+1) 778-782-3765
E-mail: dleznoff@sfu.ca

Results

Synthesis and structure: The synthesis of a series of 5,6-substituted bis(2-pyridylimino)isoindolines was accomplished by

using a one-pot reaction of 4,5-substituted phthalonitrile,[27,28] 2-aminopyridine, and calcium chloride in refluxing 1-butanol or 1-hexanol for 18–19 h (Figure 1).[29,30]

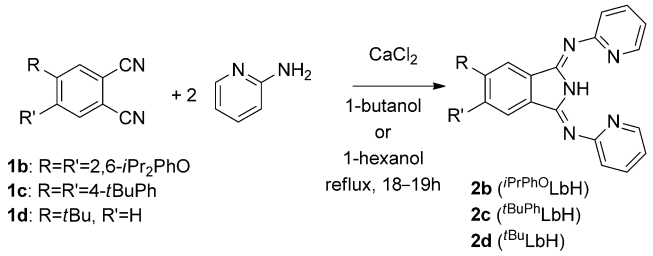

Figure 1. Synthetic procedure for a series of bis(2-pyridylimino) isoindolines **2b**–**2d**. Compound **2a** in which R = R′ = H was synthesized according to a literature procedure.[31]

Upon cooling to room temperature, crude **2b** or **2c** precipitated out of solution, was isolated by filtration and purified by recrystallization by layering hexanes onto a solution of the crude product in chloroform. However, **2d** remains in solution upon cooling of the reaction mixture and a crude solid was isolated by removing the solvent in vacuo and purified by silica gel column chromatography. Compounds **2b**–**2d** were isolated in low to moderate yields, which is partially due to the tendency of the phthalonitrile starting materials to form phthalocyanine impurities in addition to the desired products.

The identity and purity of **2b**–**2d** were determined by ^{1}H and ^{13}C NMR spectroscopy and from the elemental analysis (C, H, N). The ^{1}H NMR spectra of **2b**–**2d** all show broad singlets for the isoindoline N–H proton at $\delta = 13.63$, 13.96, and 13.88 ppm in CD_2Cl_2, respectively. The remaining resonances in the spectra are consistent with the structure and are unremarkable.

Unsubstituted bis(2-pyridylimino)isoindoline (**2a**) and **2b**–**2d** all absorb strongly in the near-UV and violet regions in chloroform with extinction coefficients on the order of $10^4\,M^{-1}cm^{-1}$ (Figure 2). The lowest energy absorption band for **2a** has an absorption maximum at 409 nm. Compound **2d** has an absorption spectrum that is similar to **2a** and also has an absorption maximum of 409 nm for the lowest energy absorption band. The lowest energy absorption bands of **2b** and **2c** are slightly red-shifted to 411 and 412 nm, respectively. Overall, consistent with these spectra, the compounds appear yellow in solution and in the solid state. This lack of absorption in the majority of the visible spectrum is important with respect to the solid-state optical birefringence measurements below.

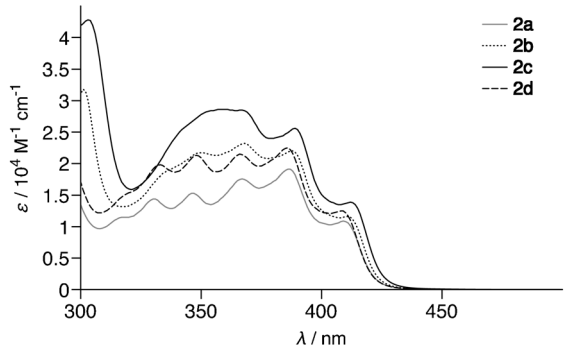

Figure 2. UV/Vis absorption spectra of **2a**–**2d** in $CHCl_3$.

Compounds **2b**–**2d** were also structurally characterized by using single-crystal X-ray diffraction. The solid-state structural data are consistent with the NMR spectra and elemental analyses. The single-crystal X-ray structure of **2a** was reported previously[31] and all bond lengths are within the expected ranges.[32] The metrical parameters of compounds **2c** and **2d** are comparable to those previously reported for **2a**: all of the bond lengths are within 0.02 Å and bond angles are within 2.5° of the reported values for **2a**.[31] Unfortunately, **2b** exhibits significant disorder in the pyridyl rings and the bond lengths of **2b** show a larger deviation from the values reported for **2a**.[31] Nevertheless, the identity and connectivity of **2b** is unambiguous (Figure 3, top left).

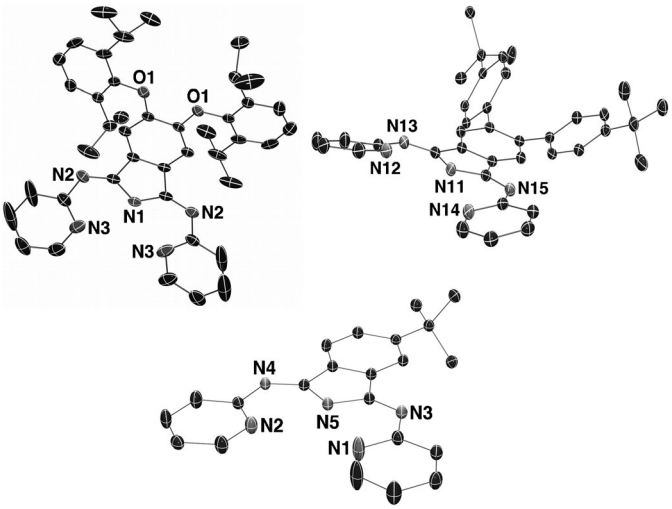

Figure 3. Molecular structures of **2b** (top left), **2c** (top right), and **2d** (bottom). Thermal ellipsoids are set at 30% probability. Hydrogen atoms have been removed for clarity.

Compound **2a** is not planar and the pyridyl rings are tilted out of the isoindoline backbone mean plane by 10°. The disorder of the pyridyl rings in **2b** makes it difficult to provide a more detailed description of the tilting of the rings. The diisopropylphenoxy substituents, however, are oriented approximately perpendicular to the isoindoline core of **2b**. Compound **2c** crystallizes with two molecules in the asymmetric unit. The 4-*tert*-butylphenyl substituents of both molecules are tilted out of the mean plane formed by the nearly planar isoindoline moieties by 44–53° due to steric repulsion between adjacent phenyl rings (Figure 3, top right). The pyridine units are also tilted out of the mean plane formed by the isoindoline backbone, but to a lesser degree (8–15°). Presumably, the tilting of the pyridine rings in **2a**–

2c is due to packing effects in the solid state, since the pyridine rings are equivalent in solution for all three compounds according to their ^{1}H and ^{13}C NMR spectra. Compound **2d** is unique in that it is planar in the solid-state (Figure 3, bottom).

Overall, the molecular solid-state structures of **2a**–**2d** are unremarkable. However, the birefringence of the crystals is determined not just from the anisotropy of the molecular polarizability but, critically, the intermolecular solid-state packing; this packing is, of course, influenced by the molecular conformation and overall planarity.

Intermolecular packing and birefringence: When examining the birefringence of molecular crystals, such as those discussed in this paper, it is very important to take into consideration both the shape of the individual molecules as well as how they pack and orient themselves with respect to one another in the overall crystal structure; these are standard concepts in organic crystal engineering.[33–35] These considerations can be aided by examining the Lorentz–Lorenz equation, which states that the refractive index in a particular direction increases with the increase of either the polarizability in that direction, or how densely the molecules pack in the crystal structure.[3,8–10] Thus, by introducing a high anisotropy in the polarizability, the anisotropy of the refractive index (and hence birefringence) will be high. For instance, in the case of 2,2′:6′,2″-terpyridine (terpy), the individual molecules are flat and contain highly polarizable aromatic rings, which suggests a very high anisotropy in polarization,[36] a feature key to the enhancement of birefringent properties. However, when its crystal structure is viewed down the *c* axis, the molecules are oriented in a herringbone pattern, which means overall, their anisotropy is lost, resulting in a nearly isotropic arrangement overall, and a very low birefringence, whereas a face-to-face arrangement would result in a high value. For the isoindoline molecules described above, the birefringence structure–property relationship is probed below by measuring their birefringence values and interpreting them with respect to the 3D packing of the molecules.[37]

Birefringence of ***2a***: Since **2a** crystallizes in an orthorhombic space group, with the (001), or (*ab*), plane as the primary face, one of the principle birefringence values (i.e., Δn_{ab}) was determined. The birefringence of **2a** was found to be a modest, but still significant $\Delta n_{ab} = 0.0654(3)$ in this plane. The polarizabilities in each direction are important, but in particular those in the plane perpendicular to the direction of view will determine Δn down that crystal face. Accordingly, Figure 4 (top) presents a view of the crystal structure as viewed perpendicularly to the (001) plane (i.e., along the *c* axis). Here, the orientation of the individual flat molecules of **2a** is difficult to examine, therefore when the crystal structure is viewed along the *b* axis (perpendicular to the direction of measurement), it can be seen that the molecules are tilted 45° from the *c* axis, as shown in Figure 4 (bottom). Thus, the component of the light's electric field along the

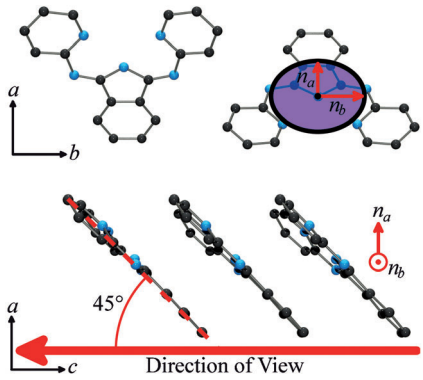

Figure 4. View of the crystal structure of **2a** in the (001) plane (top) and (010) plane (bottom). The slice of the optical indicatrix measured is shown. N atoms are shown in blue and C atoms in black.

b axis experiences the maximum polarizability of a molecule of **2a**, while the component along the *a* axis experiences a smaller, but still significant projection of the molecule's polarizability, thus a small birefringence value is observed. If the component of the field along the *a* axis felt the full polarizability of the molecule (i.e., if the molecule were oriented 90° to the *c* axis, not 45°), then the birefringence in the *ab* plane would likely approach zero and Δn in the *ac* or *bc* planes would be much higher. Hence, ideally, to maximize the birefringence, the molecules should be at 0° to (i.e., aligned with) the direction of view. These considerations are consistent with the 2D slice of the optical indicatrix (an ellipsoidal plot of the value of the refractive index in 3D) shown in Figure 4.

Birefringence of ***2b***: In the solid state, molecules of **2b** form head-to-tail chains along the *b* axis that stack along the *a* axis with intermolecular π–π distances of 6.78 Å. The much larger π–π distance in comparison to **2c** and **2d** (discussed below) is likely enforced by the steric bulk of the diisopropylphenoxy substituents. Unlike **2a**, **2b** crystallizes in a monoclinic space group with (110) as the primary face, which means that none of the principle birefringence values are measureable. Instead, an oblique slice of the optical indicatrix is observed. The birefringence of this slice is therefore denoted as $\Delta n_{(110)} = n' - n''$, in which n' and n'' are the major axes of this slice of the indicatrix. For **2b**, this value was found to be $\Delta n_{(110)} = 0.0629(17)$, with $n' = 1.713(2)$ and $n'' = 1.651(2)$. Figure 5 (top) presents a view of this face. What is seen here is very similar to **2a**: a set of layered molecules oriented at an angle to the primary face. From this figure, the birefringence can already be expected to be small. When the structure is viewed perpendicularly to this direction (Figure 5, bottom), it is revealed that the molecules are oriented 35°. This angle being slightly smaller than that in **2a**, one would expect a higher birefringence value, but upon closer inspection, it is seen that the molecules are also slightly out of alignment in the n' direction as well. This, in combination with the polarizability contribution of the nearly perpendicular *i*PrPhO groups is consistent with

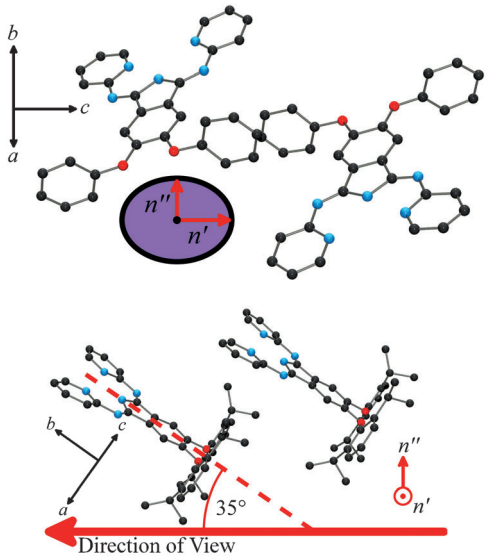

Figure 5. View of the crystal structure of **2b** in the (110) plane (top) and a perpendicular plane (bottom). The slice of the optical indicatrix measured is shown. N atoms are shown in blue, C atoms in black, and O atoms in red.

the observation of a birefringence value similar to that for **2a**.

Birefringence of ***2c***: Molecules of **2c** pack in such a way as to align themselves in parallel layers as well as stack in columns along the *c* axis. These stacks form slanted columns with average intermolecular π–π distances of 3.85 Å. Compound **2c** crystallizes in a triclinic space group, with $(01\bar{1})$ as the primary face, and a very high value of $\Delta n_{(01\bar{1})} = 0.588(10)$ was determined for the birefringence in this plane. When viewed perpendicularly to $(01\bar{1})$, as in Figure 6 (top), a layered structure can be seen, in which the molecules of **2c** are aligned nearly perpendicularly to this plane, and the direction of highest polarizability is in the *n*′ direction. This alignment is what likely gives rise to the very large birefringence value observed. A clearer picture of this system is shown in the lower panel of Figure 6. This presents a perpendicular view to that shown in the upper panel of Figure 6. As shown, the molecules of **2c** are aligned at 25° to the direction of view. Although this is much shallower than in **2a**, which is consistent with its much higher birefringence value, the difference between the angles of this compound and **2b** is not large, yet a huge jump in birefringence is seen. It is clear that other factors must be involved in this leap. For instance, the bulky *i*PrPhO groups create a larger spacing between molecules (as seen in comparing the π–π distances), resulting in a lower density, one of the key factors in refractive index value. It is likely that this, in combination with the slight tilt in **2b** discussed above results in a seemingly low value for **2b**, compared with **2c**.

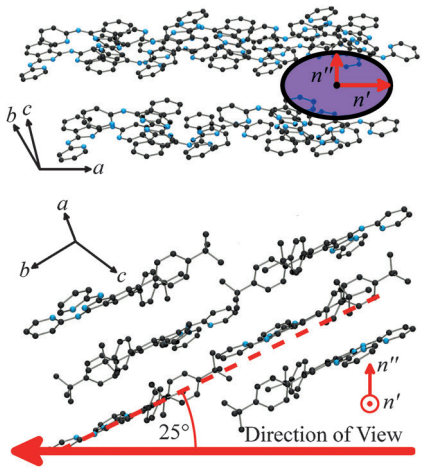

Figure 6. View of the crystal structure of **2c** in the $(01\bar{1})$ plane (top) and a perpendicular plane (bottom). The slice of the optical indicatrix measured is shown. N atoms are shown in blue and C atoms in black.

Birefringence of ***2d***: Molecules of **2d** align themselves to form parallel layers. Within these layers, each molecule stacks to form columns along the *c* axis with short intermolecular π–π distances of 3.39 Å (Figure 7). As with **2a**, compound **2d** crystallizes in an orthorhombic space group, but with (010) as the primary face. However, the **2d** molecules align themselves with the direction of view (i.e., at 0°), which, along with the short π–π distance implies that the primary birefringence value, Δn_{ac}, should be very high. Indeed, when measured, the value is found to be $\Delta n_{ac} = 0.701(12)$, the highest of those reported among **2a**–**2d**. Note that **2a**–**2d** have nearly identical UV/Vis spectra and thus the wide range of Δn values, including the very large value for **2d**, is not attributable to apparent Δn inflations due to measurements near absorption bands.[15]

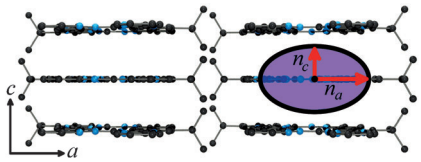

Figure 7. View of the crystal structure of **2d** in the (010) plane. The slice of the optical indicatrix measured is shown. N atoms are shown in blue and C atoms in black.

Discussion

In lobsterate **2a** and the three new lobsterate-based molecules (**2b**–**2d**) synthesized here, we have illustrated how heavily the orientation and arrangement of individual units in a molecular crystal impact the birefringence. By varying one aspect of the molecule, and hence how the molecules collectively pack in the solid state, birefringence values ranging across an order of magnitude (0.06–0.7) were obtained. This trend is also seen in the literature, with birefrin-

gence values for solid materials ranging from isotropic ($\Delta n = 0$) to very high ($\Delta n > 0.6$),[11,38–45] However, only a handful have a value greater than 0.3 (with many of them less than 0.1), despite containing highly polarizable aromatic moieties. The fact that these values vary so wildly stresses the importance of the crystallographic arrangement when a high value of birefringence is desired. For example, picric acid is a planar aromatic compound, which should have a very high polarizability in the plane and low polarizability perpendicular to the plane, however, its birefringence value is an unremarkable $\Delta n_{ac} = 0.06$.[46] Much like **2a** and **2b** (which have similar values), the picric acid molecules orient themselves in a herringbone pattern in their crystal structure, and are not near parallel to the direction of view. However, ammonium picrate (the anion of which has the same molecular polarizability anisotropy as picric acid) has a much larger birefringence value of $\Delta n_{ac} = 0.419$.[46,47] The addition of the ammonium cations causes this material to favor a much better aligned structure, in which the picrate molecules are oriented near face-to-face, and are near parallel to the direction of view, similar to **2c**. This type of analysis suggests that modern crystal-engineering concepts could be harnessed to maximize preferred supramolecular orientations for generating high Δn materials.

Conclusion

This structure–birefringence property analysis of **2a** and its derivatives has clearly demonstrated the importance of several factors which affect the birefringence values of solids. These include:

1) The anisotropic polarizability of the molecules.
2) Supramolecular orientation of the molecules in the unit cell.
3) The primary growth face.

Optical transparency at the wavelength of measurement is also an important consideration. The first point above is illustrated especially well in **2c** and **2d**, for which a highly anisotropic polarizability is the critical factor. Without this feature, the relative orientation of the molecules would have little effect. This alone, however, is insufficient for a high birefringence value. All of the molecules examined here have similar molecular polarizability anisotropies, yet the differences in birefringence vary widely. Ideally, for aromatic ligands, such as these lobsterates, the molecules would be aligned face-to-face (the second point, above). This is the case for **2c** and **2d**, hence their very high Δn values. Finally, a crystal may have a very large birefringence in one plane, but it may not be observable if the crystals do not grow with that face as the primary (largest) face.

One other factor to consider is density. With a lower packing density, the refractive indices will also decrease (as per the Lorentz–Lorenz equation). This is likely another important factor leading to the low value for **2b**, and potentially aids in generating the high values of **2c** and **2d**. The impact on Δn of controlling density in a systematic fashion through crystal engineering deserves further attention.

Through these analyses, an improved understanding of the impact of the solid-state 3D structure on birefringence values was targeted, thereby providing a basis for interpreting the large body of organic crystal birefringence data[11] at the molecular packing level, as well as facilitate molecular and crystal-engineering design principles[33–35] to generate highly birefringent materials. With all of these features in mind, we have started incorporating these ligands in combination with a coordination polymer framework with the goal of reaching higher birefringence values.

Experimental Section

General: Anhydrous calcium chloride was stored, weighed out, and transferred to reaction flasks under a dinitrogen atmosphere in a MBraun Labmaster 130 glovebox. All reflux reactions were carried out under a dinitrogen atmosphere using standard Schlenk techniques. Isolation of the products was conducted in air.

Compounds **1b**[27] and **1c**[28] were synthesized according to reported procedures. Compound **2a** was synthesized using a literature procedure.[31] Compounds **2b**–**2d** were synthesized using procedures adapted from published literature methods.[29,30] Anhydrous calcium chloride (≥96.0%), anhydrous 1-hexanol (≥99%), anhydrous 1-butanol (99.8%) and all other reagents were obtained from commercial sources and used as received.

^{1}H and ^{13}C NMR spectra were collected on a Bruker AVANCE II digital NMR spectrometer with a 5 mm QNP cryoprobe operating at 600 MHz for ^{1}H spectra. Chemical shifts for ^{1}H NMR spectra were referenced to residual ^{1}H NMR resonances of the deuterated solvent and ^{13}C NMR spectra were referenced to ^{13}C NMR resonances of the deuterated solvent. All chemical shifts are reported relative to tetramethylsilane.

All UV/Vis absorption spectra were recorded on a Varian Cary 5000 Spectrophotometer in a 0.1 cm quartz cell at room temperature. UV/Vis samples were prepared as 0.33 mM stock solutions (50 mL) in chloroform.

Elemental analyses (C, H, N) were performed by Mr. Farzad Haftbaradaran at Simon Fraser University on a Carlo Erba EA 1110 CHN elemental analyzer.

Synthesis of 1,3-bis(2-pyridylimino)-5,6-bis(2,6-diisopropylphenoxy)isoindoline (2b): A mixture of 4,5-bis(2,6-diisopropylphenoxy)phthalonitrile

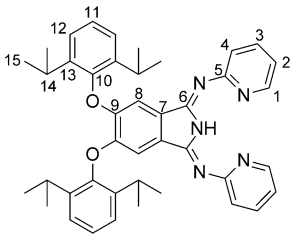

(2.8711 g, 5.973 mmol), 2-aminopyridine (1.2928 g, 13.74 mmol), and $CaCl_2$ (0.3315 g, 2.987 mmol) was heated to reflux in 1-butanol (20 mL) for 18 h to give a purple reaction mixture. The reaction mixture was cooled to room temperature and a yellow solid with green and purple impurities was collected by vacuum filtration, washed with hexanes, and air dried. The crude product was dissolved in chloroform, filtered through celite, and recrystallized by layering hexanes over the chloroform solution in test tubes. Yellow crystals of **2b** were collected by vacuum filtra-

tion, washed with hexanes, and air dried. A second small batch of crystals can be obtained by repeating the crystallization procedure on the filtrate. Yield: 2.587 g (66.44%); m.p. >300°C; ^{1}H NMR (600 MHz, CD_2Cl_2, 298 K): δ=1.24 (br m, 26H; CH*Me*$_2$), 3.21 (septet, J=7 Hz, 4H; C*H*Me$_2$), 6.98 (s, 2H; *H*-8), 7.08 (m, 2H; *H*-2), 7.29 (m, 2H; *H*-4), 7.36 (m, 6H; *H*-11 and *H*-12), 7.71 (m, 2H; *H*-3), 8.55 (m, 2H; *H*-1), 13.63 ppm (br s, 1H; N*H*); ^{13}C{^{1}H} NMR (151 MHz, CD_2Cl_2, 298 K): δ= 22.9 (*C*-15), 24.6 (*C*-15), 28.0 (*C*-14), 107.7 (*C*-8), 120.5 (*C*-2), 123.4 (*C*-4), 125.4 (*C*-12), 127.0 (*C*-11), 130.2 (*C*-7), 138.6 (*C*-3), 142.1 (*C*-13), 148.3 (*C*-1), 149.1 (*C*-10), 152.0 (*C*-9), 153.7 (*C*-6), 161.1 ppm (*C*-5); elemental analysis calcd (%) for $C_{42}H_{45}N_5O_2$: C 77.39, H 6.96, N 10.74; found: C 77.06, H 6.88, N 10.51.

Synthesis of 1,3-bis(2-pyridylimino)-5,6-bis(4-*tert*-butylphenyl)isoindoline (2c): A mixture of 4,5-bis(4-*tert*-butylphenyl)phthalonitrile (1.996 g,

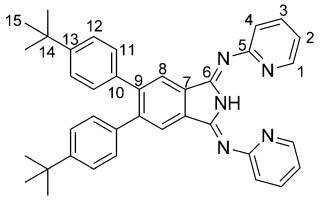

5.085 mmol), 2-aminopyridine (1.101 g, 11.69 mmol), and $CaCl_2$ (0.282 g, 2.54 mmol) was heated to reflux in 1-hexanol (20 mL) for 18 h to give a green mixture. A yellow solid precipitated out of the reaction mixture as it cooled to room temperature. The yellow solid was collected by vacuum filtration, washed with hexanes, and air dried. The crude product was dissolved in chloroform, gravity filtered and then recrystallized by layering hexanes over the chloroform solution in test tubes. Yellow crystals of **2c** were collected by vacuum filtration, washed with hexanes, and air dried. The solvent was removed from the filtrate under reduced pressure and a second batch of yellow crystals was obtained by repeating the recrystallization process. Yield: 1.119 g (39.04%); m.p. 298°C; ^{1}H NMR (600 MHz, CD_2Cl_2, 298 K): δ=1.31(s, 18H; *t*Bu), 7.15 (m, 2H; *H*-2), 7.18 (m, 4H; *H*-11), 7.30 (m, 4H; *H*-12), 7.42 (m, 2H; *H*-4), 7.79 (m, 2H; *H*-3), 8.06 (s, 2H; *H*-8), 8.65 (m, 2H; *H*-1), 13.96 ppm (br s, 1H; N*H*); ^{13}C{^{1}H} NMR (151 MHz, CD_2Cl_2, 298 K): δ=31.6 (*C*-15), 34.9 (*C*-14), 120.8 (*C*-2), 123.8 (*C*-4), 125.0 (*C*-8), 125.4 (*C*-12), 130.0 (*C*-11), 135.2 (*C*-7), 138.6 (*C*-10), 138.7 (*C*-3), 145.1 (*C*-9), 148.5 (*C*-1), 150.7 (*C*-13), 154.0 (*C*-6), 161.1 ppm (*C*-5); elemental analysis calcd (%) for $C_{38}H_{37}N_5$: C 80.96, H 6.62, N 12.42; found: C 80.69, H 6.59, N 12.25.

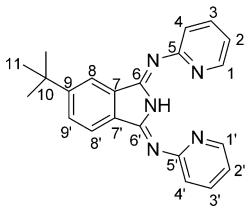

Synthesis of 1,3-bis(2-pyridylimino)-5-*tert*-butylisoindoline (2d): A mixture of 4-*tert*-butylphthalonitrile (1.658 g, 9.000 mmol), 2-aminopyridine (1.788 g, 19.00 mmol), and $CaCl_2$ (0.499 g, 4.50 mmol) was heated to reflux in 1-butanol (25 mL) for 19 h to give a pale green mixture. The solvent was removed by vacuum distillation and the green oil was dissolved in chloroform and washed with water. The organic layer was collected and concentrated under reduced pressure. The green impurity was separated from the product by silica gel column chromatography (50:1 $CHCl_3$/CH_3OH followed by 40:1 $CHCl_3$/CH_3OH then 25:1 $CHCl_3$/CH_3OH). X-ray quality crystals were obtained by layering water under a concentrated ethanol solution of the purified product. The yellow crystals of **2d** were collected by vacuum filtration, washed with water, and dried under vacuum at 80°C. Yield: 0.875 g (27.4%); m.p. 127°C; ^{1}H NMR (600 MHz, CD_2Cl_2, 298 K): δ=1.45 (s, 9H; *t*Bu), 7.14 (m, 2H; *H*-2 and *H*-2′), 7.43 (m, 2H; *H*-4 and *H*-4′), 7.73 (m, 1H; *H*-9′), 7.79 (m, 2H; *H*-3 and *H*-3′), 7.95 (m, 1H; *H*-8′), 8.08 (m, 1H; *H*-8), 8.62 (m, 2H; *H*-1 and *H*-1′), 13.88 ppm (br s, 1H; N*H*); ^{13}C{^{1}H} NMR (151 MHz, CD_2Cl_2, 298 K): δ=31.70 (*C*-11), 36.01 (*C*-10), 119.78 (*C*-8), 120.65/120.70 (*C*-2 and *C*-2′), 122.58 (*C*-8′), 123.61/123.62 (*C*-4 and *C*-4′), 129.77 (*C*-9′), 133.85 (*C*-7′), 136.48 (*C*-7), 138.65/138.67 (*C*-3 and *C*-3′), 148.41/148.45 (*C*-1 and *C*-1′), 154.09 (*C*-6′), 154.39 (*C*-6), 156.49 (*C*-9), 161.14/161.19 ppm (*C*-5 and *C*-5′); elemental analysis calcd (%) for $C_{22}H_{21}N_5$: C 74.34, H 5.96, N 19.70; found: C 74.51, H 5.82, N 19.40.

X-ray crystallography: Crystallographic data for **2b**–**2d** are listed in Table 1. A crystal suitable for data collection was selected and mounted in Paratone oil on a MiTeGen head, then placed in the cold stream (100 K) of the diffractometer. Data were collected on a Bruker SMART6000 diffractometer with $Cu_{K\alpha}$ radiation using ω and ϕ scans for complete coverage. The data were then processed using SAINT (Bruker AXS, v6.26 A) and corrected for absorption using SADABS (Bruker AXS v2.03).

Table 1. Crystallographic data for **2b**, **2c**, and **2d**.

	2b	**2c**	**2d**
formula	$C_{42}H_{45}N_5O_2$	$C_{38}H_{37}N_5$	$C_{22}H_{21}N_5$
formula weight	651.85	563.74	355.44
crystal system	monoclinic	triclinic	orthorhombic
space group	*C*2/*c*	$P\bar{1}$	*Pbcm*
a [Å]	14.6097(2)	11.8199(4)	13.4118(3)
b [Å]	13.1038(2)	16.8456(5)	20.0522(4)
c [Å]	19.5557(3)	18.3027(5)	6.7768(2)
α [°]	90	111.7740(10)	90
β [°]	92.6030(10)	94.227(2)	90
γ [°]	90	108.673(2)	90
V [Å^3]	3739.93(10)	3128.49(18)	1822.53(8)
Z	4	4	4
T [K]	100(2)	100(2)	100(2)
ρ_{calcd} [g cm^{-3}]	1.158	1.197	1.295
μ [mm^{-1}]	0.565	0.550	0.627
reflns collected	3324	10852	1812
significant reflns	3218	10152	1714
R [$I_o \geq 2.5\sigma(I_o)$]	0.0811	0.0480	0.0426
R_w [$I_o \geq 2.5\sigma(I_o)$]	0.0893	0.0542	0.0683
goodness of fit	1.0994	1.0898	0.8964

The structures were solved using direct methods (SIR92)[48] and refined by least-squares procedures using CRYSTALS.[49] Hydrogen atoms were placed in idealized geometric positions and linked to their respective carbon atoms using a riding model during refinement. The isotropic temperature factor of each hydrogen atom was initially set to 1.2 times that of the carbon atom it is bonded to and then the temperature factors of groups of similar hydrogen atoms were linked during refinement. Compound **2b** exhibited disorder of the entire molecule over two positions as well as significant disorder of the pyridyl moieties in multiple conformations that could not be accounted for, which resulted in irregular ellipsoid shapes throughout the entire molecule. Crystal structure diagrams were generated using ORTEP-3 for Windows (v. 2.02)[50] and rendered using POV-Ray (v. 3.6.1c).[51]

CCDC-848830 (**2b**), 848829 (**2c**), and 848828 (**2d**) contain the supplementary crystallographic data for this paper. These data can be obtained free of charge from The Cambridge Crystallographic Data Centre via www.ccdc.cam.ac.uk/data_request/cif.

Birefringence measurements: Optical retardation and crystal thickness measurements were made on plate-shaped crystals of **2a**, **2c** and **2d** by means of polarized light microscopy using an Olympus BX60 microscope with a U-CTE Berek compensator (**2a**) and a U-CTB thick Berek compensator (**2c** and **2d**) at λ=546 nm at room temperature. The birefringence was calculated by dividing the retardation by the thickness. The orientation of the slice of the optical indicatrix in the viewing plane was determined using single-crystal X-ray diffraction techniques.

The refractive index, and its dependence on crystal orientation, of **2b** was determined by using a Metricon Model 2010/M Prism Coupler at λ= 1552 nm. The refractive index was measured as the crystal was rotated about the normal to the measurement plane from θ=0–120° in 10° incre-

ments (collection of further data points was precluded by crystal destruction). The data were fit to Equation (1), in which $n(\theta)$ is the orientation-dependent refractive index, $2A = \Delta n_{(hkl)}$ is the difference between the maximum and minimum refractive indices (i.e., the birefringence in the (hkl) plane), δ is the relative phase between the instrument and crystal axes and $\bar{n}$ is the average refractive index.

$$n(\theta) = A\cos\left(\frac{\theta}{\pi} - \delta\right) + \bar{n} \quad (1)$$

Acknowledgements

The authors gratefully acknowledge financial support provided by the Natural Sciences and Engineering Research Council of Canada, Natural Resources Canada, and Simon Fraser University. We thank Dr. James F. Britten and Dr. Hilary Jenkins at McMaster University for assistance with X-ray crystallography.

[1] P. Velasquez, M. del Mar Sánchez-López, I. Moreno, D. Puerto, F. Mateos, *Am. J. Phys.* **2005**, *73*, 357.
[2] S. Saeed, P. J. Bos, Z. Li, *Jpn. J. Appl. Phys. Part 1* **2001**, *40*, 3266.
[3] S. G. Lipson, H. Lipson, D. S. Tannhauser, *Optical Physics*, 3rd ed., Cambridge University Press, Cambridge, U.K., **1995**.
[4] S.-T. Wu, C.-S. Wu, *Appl. Phys. Lett.* **1996**, *68*, 1455.
[5] M. Schadt, *Jpn. J. Appl. Phys.* **2009**, *48*, 03B001.
[6] H. L. Ong, *Appl. Phys. Lett.* **1991**, *59*, 155.
[7] M. J. Weber, *Handbook of Optical Materials*, CRC Press, Boca Raton, FL, **2003**.
[8] R. E. Newnham, *Structure–Property Relations*, Springer, New York, **1975**.
[9] R. E. Newnham, *Properties of Materials: Anisotropy, Symmetry, Structure*, Oxford University Press, New York, **2005**.
[10] E. Hecht, *Optics*, 4th ed., Addison Wesley, San Francisco, **2002**.
[11] A. N. Winchell, *The Optical Properties of Organic Compounds*, Academic Press, New York, **1954**.
[12] E. T. Wherry, *J. Wash. Acad. Sci.* **1918**, *8*, 277.
[13] R. G. Hunsperger, *Integrated Optics: Theory and Technology*, Springer, New York, **2009**.
[14] Most of the very high birefringence values are for crystals that are highly colored dyes, and since the refractive index of a material at a wavelength close to an absorption band changes enormously versus the transparent region, these measurements should be viewed with a great deal of caution; see reference [15].
[15] S. H. Simpson, R. M. Richardson, S. Hanna, *J. Chem. Phys.* **2007**, *127*, 104901.
[16] B. Kahr, J. Freudenthal, E. Gunn, *Acc. Chem. Res.* **2010**, *43*, 684.
[17] W. Kaminsky, K. Claborn, B. Kahr, *Chem. Soc. Rev.* **2004**, *33*, 514.
[18] S. R. Batten, S. M. Neville, D. R. Turner, *Coordination Polymers: Design, Analysis and Application*, RSC, Cambridge (UK), **2009**.
[19] *Metal–Organic Frameworks: Design and Application* (Ed.: L. R. MacGillivray), Wiley, New Jersey, **2010**.
[20] *Design and Construction of Coordination Polymers* (Eds.: M.-C. Hong, L. Chen), Wiley, New Jersey, **2009**.
[21] J. S. Ovens, A. R. Geisheimer, A. A. Bokov, Z.-G. Ye, D. B. Leznoff, *Inorg. Chem.* **2010**, *49*, 9609.
[22] M. J. Katz, D. B. Leznoff, *J. Am. Chem. Soc.* **2009**, *131*, 18435.
[23] M. J. Katz, H. Kaluarachchi, R. J. Batchelor, A. A. Bokov, Z.-G. Ye, D. B. Leznoff, *Angew. Chem.* **2007**, *119*, 8960; *Angew. Chem. Int. Ed.* **2007**, *46*, 8804.
[24] N. D. Draper, R. J. Batchelor, B. C. Sih, Z.-G. Ye, D. B. Leznoff, *Chem. Mater.* **2003**, *15*, 1612.
[25] C. A. Bessel, R. F. See, D. L. Jameson, M. R. Churchill, K. J. Takeuchi, *J. Chem. Soc. Dalton Trans.* **1992**, 3223.
[26] K. F. Bowes, I. P. Clark, J. M. Cole, M. Gourlay, A. M. E. Griffin, M. F. Mahon, L. Ooi, A. W. Parker, P. R. Raithby, H. A. Sparkes, M. Towrie, *CrystEngComm* **2005**, *7*, 269.
[27] N. B. McKeown, S. Makhseed, K. J. Msayib, L.-L. Ooi, M. Helliwell, J. E. Warren, *Angew. Chem.* **2005**, *117*, 7718; *Angew. Chem. Int. Ed.* **2005**, *44*, 7546.
[28] S. Eu, T. Katoh, T. Umeyama, Y. Matano, H. Imahori, *Dalton Trans.* **2008**, *40*, 5476.
[29] W. O. Siegl, *J. Org. Chem.* **1977**, *42*, 1872.
[30] B. Langlotz, H. Wadepohl, L. Gade, *Angew. Chem.* **2008**, *120*, 4748; *Angew. Chem. Int. Ed.* **2008**, *47*, 4670.
[31] W. Schilf, *J. Mol. Struct.* **2004**, *691*, 141.
[32] F. H. Allen, O. Kennard, D. G. Watson, L. Brammer, A. G. Orpen, R. Taylor, *J. Chem. Soc. Perkin Trans. 2* **1987**, *12*, S1.
[33] K. Biradha, C.-Y. Su, J. J. Vittal, *Cryst. Growth Des.* **2011**, *11*, 875.
[34] C. B. Aakeröy, N. R. Champness, C. Janiak, *CrystEngComm* **2010**, *12*, 22.
[35] D. Das, G. Desiraju, *CrystEngComm* **2006**, *8*, 674.
[36] S. B. Bulgarevich, D. V. Bren, D. Y. Movshovich, S. E. Filippov, E. P. Olekhnovich, I. V. Korobka, *Russ. J. Gen. Chem.* **2002**, *72*, 1446.
[37] R. R. Tykwinski, U. Gubler, R. E. Martin, F. Diederich, C. Bosshard, P. Günter, *J. Phys. Chem. B* **1998**, *102*, 4451.
[38] R. N. Castle, N. F. Witt, C. F. Poe, *J. Am. Chem. Soc.* **1949**, *71*, 228.
[39] R. N. Castle, *Mikrochim. Acta* **1951**, *38*, 92.
[40] R. N. Castle, *Mikrochim. Acta* **1953**, *40*, 196.
[41] R. N. Castle, *J. Am. Pharm. Assoc.* **1952**, *41*, 143.
[42] R. N. Castle, *Mikrochim. Acta* **1955**, *43*, 761.
[43] J. A. Biles, *Mikrochim. Acta* **1952**, *39*, 69.
[44] W. Bryant, *Microscope* **1976**, *24*, 261.
[45] W. Bryant, *Microscope* **1992**, *40*, 153.
[46] J. Mitchell Jr., W. M. D. Bryant, *J. Wash. Acad. Sci.* **1943**, *33*, 128.
[47] H. E. Merwin, *J. Wash. Acad. Sci.* **1919**, *9*, 429.
[48] A. Altomare, G. Cascarano, C. Giacovazzo, A. Guagliardi, *J. Appl. Crystallogr.* **1993**, *26*, 343.
[49] P. W. Betteridge, J. R. Carruthers, R. I. Cooper, K. Prout, D. J. Watkin, *J. Appl. Crystallogr.* **2003**, *36*, 1487.
[50] L. J. Farrugia, *J. Appl. Crystallogr.* **1997**, *30*, 565.
[51] Persistance of Vision Pty., *Persistance of Vision (TM) Raytracer*, Persistance of Vision Pty., Williamstown, Victoria, Australia, **2004**.

Received: October 31, 2011
Published online: ■■ ■■, 0000

Birefringence

E. W. Y. Wong, J. S. Ovens,
*D. B. Leznoff** ..... ▮▮▮▮–▮▮▮▮

From Low to Very High Birefringence in Bis(2-pyridylimino)isoindolines: Synthesis and Structure–Property Analysis

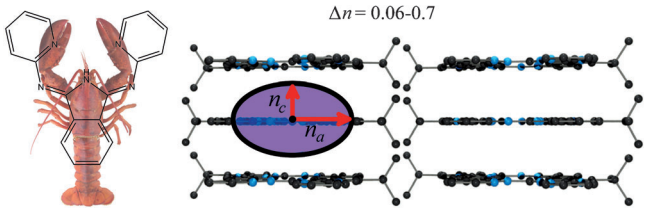

Lobsterates! Three bis(2-pyridylimino)isoindoline (lobsterate) derivatives were synthesized and structurally characterized. The birefringence (Δn) values of these (including the parent lobsterate) were measured, yielding Δn values of 0.06–0.7. These are correlated with the orientation and 3D packing of the molecules in their crystal structure, providing a framework for interpreting birefringence data of known organic molecules.